

## **MAGNETIC PROPERTIES EVOLUTION IN YTTRIUM IRON GARNET: TREND OF SINGLE-SAMPLE AND MULTI-SAMPLE SINTERING**

N. Rodziah<sup>1,\*</sup>, M. Hashim<sup>1,2</sup>, I. R. Idza<sup>1</sup>, I. Ismayadi<sup>1</sup>, A. N. Hapishah<sup>1</sup>, A. R. Norailiana<sup>1</sup>, M. Masni<sup>1</sup>, M.I. Fadzidah<sup>2</sup>, G. H. Bahmanrokh<sup>1</sup>, and M. S. E. Shafee<sup>2</sup>

<sup>1</sup>*Department of Physics, Universiti Putra Malaysia Serdang,  
43400, Serdang, Selangor, Malaysia.*

<sup>2</sup>*Advanced Materials and Nanotechnology Laboratoty, Institute of Advanced  
Technology, Universiti Putra Malaysia Serdang, 43400, Serdang, Selangor, Malaysia.*

*Corresponding author: rodzienaz@gmail.com*

### **ABSTRACT**

The influence of sintering scheme on the evolution of magnetic and morphological properties in polycrystalline Yttrium Iron Garnet (YIG) has been investigated. The samples were prepared by using High Energy Ball Milling (HEBM) technique followed by 2 different sintering schemes: (1) single-sample; (2) multi-samples; both sintered from 600<sup>0</sup>C up to 1400<sup>0</sup>C. The samples have been characterized on its phase purity, grain size distribution and B-H loop; and the relationships among these factors have been analyzed during its evolution. With great experimental care, both the single-sample and multi-sample sintering batches yielded highly similar variation of magnetic properties vs microstructure of YIG. The results show that clearly evolution of hysteresis behaviour and complex permeability is attributed to the improvement of phase purity and grain size distribution with increment of sintering temperature. 3 different groups were apparent in the B-H hysteresis loop, indicates a 3 different types of magnetism-dominancy: weak, moderate and strong ferromagnetism. That well-defined B-H loop shape was observable only when sufficient single-phase purity and crystallinity and also a sufficiently high volume fraction of grains with diameters >0.5 $\mu$ m (multe-sample sintering) or >0.6  $\mu$ m (single-sample sintering) were attained.

*Keywords: Soft Ferrimagnetic Material; Yttrium Iron Garnet; Magnetic Properties; Morphological Properties*

### **INTRODUCTION**

Rare-earth iron garnet and substituted-rare earth garnets such as Yttrium Iron Garnet (YIG), are equally important materials as compared to spinel ferrites in the microwave frequency range technology. A superior low-energy loss has made them a very promising candidate for microwave devices than the latter ones. Several investigations in properties of YIG such as structural, magnetic properties and mechanical properties have been reported in literatures [1-3], which have been focused only on the final

product sintered at high sintering temperature (>1000<sup>0</sup>C). However, no such reports have been found which focusing on the relationships between the microstructure and magnetic properties at intermediate sintering temperature, largely neglecting their parallel evolutions. A study by [4] showed that calcining treatment in temperatures influenced significantly the final microstructure, density and magnetic properties of the sintered ferrite. Hence, in this research, we attempted to investigate the composition-microstructure-magnetic properties evolutions at various intermediate sintering conditions and to observe the evolution as they developed using normal sintering and rarely single-sample sintering.

## METHOD

Appropriate high-purity powders (>99%) were weighed and mixed in an Agate Mortar according to below stoichiometric reaction:



The powder mixture was then milled for 2 hours by using high-energy ball milling (HEBM) technique in a SPEX D8000 mechanical alloying machine. Toroidal compact samples were then fabricated from the milled powder and sintered in an ambient air condition for 10 hours. Two sintering procedures were adopted:

- (1) One sample sintered at 9 different temperatures (single-sample sintering)
- (2) Nine samples, each sintered only once at different temperature (multi-sample sintering).

The samples were characterized using transmission electron microscope (TEM), X-ray Diffraction (XRD), Scanning Electron Microscope (SEM) and Static Hysteresisgraph; each for nanometer-sized confirmation, phase determination, morphological studies and B-H hysteresis loop parameters measurement respectively.

## RESULTS AND DISCUSSION

TEM micrograph as shown in Figure 1 shows that the as-milled starting powder particles were vary inhomogeneously in the nanometer-sized range of 50~180 nm with an average particle size around 92 nm. This average particle size can be considered to be unusually small for a starting powder normally used (0.8 ~1.2  $\mu$ m) in the ferrite-production industry and even in the past research of ferrites. The inhomogeneous size of particles indicates that non-uniformity of the force of the milling media (steel balls and vials) on the powder during milling process. A fine particle size has a high surface area, contributes to a high reactivity particles, and thus could stimulate the reactions between the particles. In fact, the amount of an amorphous phase is not negligible in the nanometer-sized samples [5]. However the amorphous phase would be reduced through sintering at higher and higher temperature as grain growth leads to decrease in discontinuity of the samples by reducing the number of grain boundaries. Therefore, better crystallinity and magnetic ordering could be achieved in the larger grain size, results in higher magnetization [6].

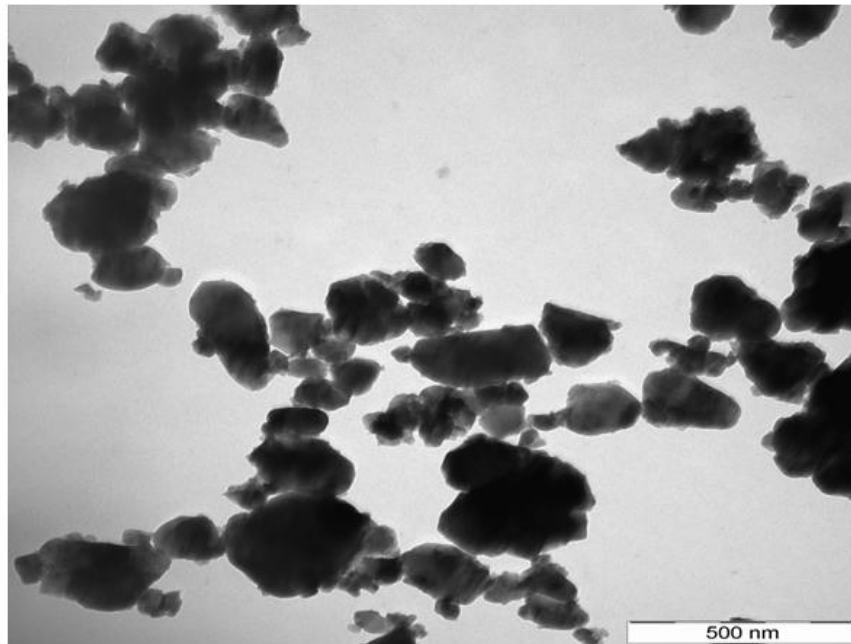


Figure 1: TEM image of a starting raw material after 2 hours of milling time

Figure 2(a) and Figure 2(b) below show the multi-plot of XRD data, illustrates the evolution of phase formation before and after sintered at 600<sup>0</sup>C up to 1400<sup>0</sup>C. As can be observed through the XRD spectra for both multi-sample and single-sample sintering samples, no reaction between the starting powders occurred prior to sintering as well as after sintering at 600<sup>0</sup>C. The reaction only started after sintering at 700<sup>0</sup>C. This indicates that crystalline YIG (Y<sub>3</sub>Fe<sub>5</sub>O<sub>12</sub>) could not be formed through milling alone due to a short period of time or at too low sintering temperatures. At 800<sup>0</sup>C for single-sample sintering samples and to 1000<sup>0</sup>C for multi-sample sintering samples, YIG phase appeared and there existed along a mixture of non magnetic secondary phases which were Yttrium Orthoferrite (YFeO<sub>3</sub>), hematite (Fe<sub>2</sub>O<sub>3</sub>) and yttrium oxide (Y<sub>2</sub>O<sub>3</sub>). As the sintering temperature increased, these secondary phases decreased and disappeared. Both multi-sample sintering and single-sample sintering samples yielded complete YIG phase at 1100<sup>0</sup>C sintering temperature. This indicates that YIG prepared via HEBM possesses lower final sintering temperature than in the conventional ceramic processing which is normally 1573K due to higher reactivity finer-sized particles [7]. The XRD patterns also shows that the most intense of YIG peak (420) became sharper and narrower with increasing sintering temperature, indicating enhancement of crystallinity, increasing grain size and also release of internal strains. This contributes to an increment in the number of magnetic mass per unit volume and better ordered in magnetic domain, giving rise to the sample's magnetization.

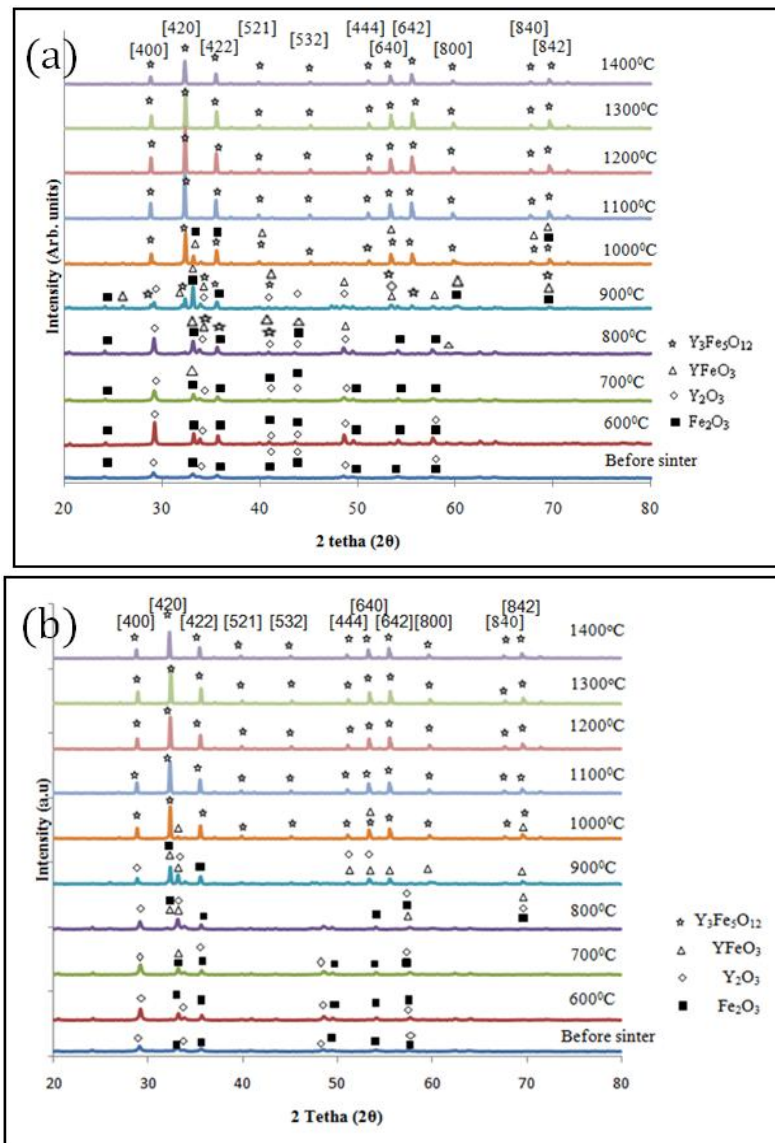


Figure 2: Multi-plot of X-ray Diffraction data for (a) single-sample sintering; (b) multi-sample sintering before and after sintered at various temperatures

SEM micrographs for single-sample and multi-sample sintering samples as shown in Figure 3 below show the evolution of polycrystalline YIG microstructure. Samples sintered from 600<sup>0</sup>C to 900<sup>0</sup>C show a rearrangement of particles and slight particle growth. After sintering at 1000<sup>0</sup>C upward, the dumbbell structure occurred through the formation of necks lead to the development of grains. At 1400<sup>0</sup>C, a hexagonal grain observed, which corresponds to the most stable condition in sintering. This leads to an increase of the grain size by diffusion during sintering process, where the evolution of grains from very fine size to a larger size would be accompanied by the evolution of magnetic ordering from superparamagnetism to ferromagnetism. Besides that, the reduction of amount of porosity and grain boundaries when sintering at higher and

higher temperature would ease the domain walls movements where those features as well as impurities would be pinning centres of domain walls movement, leads to increase the demagnetizing effects, thus decrease in the magnetization values in the samples. This description of microstructure evolution could be related to the histograms attached in the figure where the grain size distributions were plotted.

From the histograms shown below, there is a tendency to shift to the larger grain size as the sintering temperature increased. The shaded area was used as an indicator of the grain size less than 0.6  $\mu\text{m}$  (critical size for single-sample sintering samples) and 0.5 $\mu\text{m}$  (critical size for multi-sample sintering samples). By increasing the sintering temperature, the area was reduced and it was completely disappeared after the samples sintered above 1100 $^{\circ}\text{C}$ . These shows that the fraction of grain sizes larger than critical grain size was further increased with a higher sintering temperature. The number of domain walls also increased; therefore the contribution of domain wall movement to in the magnetization also increased. Furthermore, coercivity result which will be shown in B-H results later also indicates an enormous gap of the coercivity value in a transition from 1000 $^{\circ}\text{C}$  to 1100 $^{\circ}\text{C}$  to 1200 $^{\circ}\text{C}$  sintering temperatures which indicates the single domain size-critical size-multi-domain size of grains.

Table 1: Morphological properties parameter for both single-sample and multi-sample sintering at different sintering temperatures

Sintering Temperature ( $^{\circ}\text{C}$ )	Single-Sample Sintering			Multi-Sample Sintering		
	Density ( $\text{g}/\text{cm}^3$ ) $\pm 0.1$	Average Grain Size ( $\mu\text{m}$ ) $\pm 0.01$	Grain Size Distribution ( $\mu\text{m}$ )	Density ( $\text{g}/\text{cm}^3$ ) $\pm 0.1$	Average Grain Size ( $\mu\text{m}$ ) $\pm 0.01$	Grain Size Distribution ( $\mu\text{m}$ )
600	4.09	0.16	0.10-0.30	4.37	0.20	0.1-0.35
700	4.18	0.17	0.10-0.30	4.39	0.21	0.1-0.35
800	4.27	0.18	0.10-0.30	4.44	0.25	0.15-0.45
900	4.39	0.28	0.15-0.45	4.57	0.26	0.15-0.45
1000	4.51	0.33	0.15-0.70	4.59	0.28	0.15-0.60
1100	4.59	0.60	0.30-1.00	4.60	0.58	0.20-1.30
1200	4.63	1.14	0.30-2.00	4.64	0.80	0.30-2.00
1300	4.70	1.68	0.40-3.00	4.82	1.25	0.40-3.50
1400	4.74	2.71	1.00-5.00	4.86	3.09	0.50-10.00

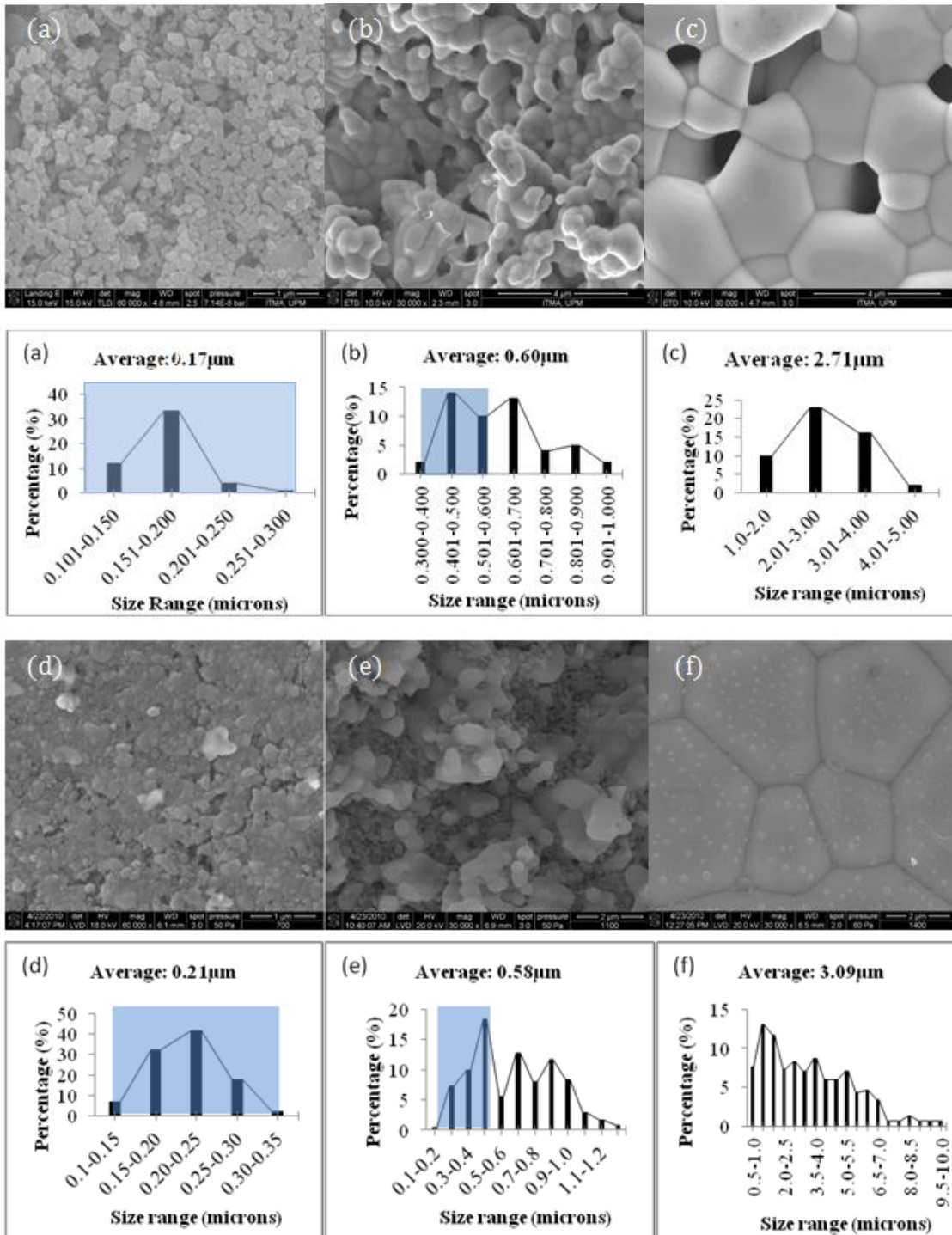


Figure 3: The SEM micrographs and grain size distributions of single-sample sintered at (a) 700<sup>o</sup>C, (b) 1100<sup>o</sup>C and (c) 1400<sup>o</sup>C and multi-sample sintered at (d) 700<sup>o</sup>C, (e) 1100<sup>o</sup>C and (f) 1400<sup>o</sup>C; which referred to three different groups of magnetism-dominancy. The shaded area in the graph refers to the single-domain grain size.

Figure 4 below shows magnetic induction, B, against magnetic field strength, H, (B-H HYsteresis loop) plotted for different sintering temperatures. Both the multi-sample and single-sample sintering samples yielded B-H hysteresis loop and indicates three evolution stages from weak to moderate to strong ferrimagnetism, as the sintering increased from 600<sup>0</sup>C to 1400<sup>0</sup>C. The XRD and SEM data above clearly explained this phenomenon. According to [8], the shape of the hysteresis loop depends on the grains in the sample. For the Group 1 samples sintered from 600<sup>0</sup>C to 900<sup>0</sup>C, the hysteresis shape was influenced by a mixture of weak ferromagnetic, paramagnetic phase and most probably some superparamagnetic phase. The narrowly bulging and linear-looking loops have very low saturation induction, B<sub>s</sub>, and coercivity, H<sub>c</sub> indicating a very small amount of ferromagnetic phase. XRD spectrum indicates that the crystalline phase was not yet dominant since there was still a large presence of the amorphous phase due to fine size grains/particles. The Group 2 of hysteresis loops refer to samples sintered at 1000<sup>0</sup>C to 1100<sup>0</sup>C (in single-sample sintering) or 1200<sup>0</sup>C (in multi-sample sintering) where a slanted sigmoid shape has been observed. There was significantly higher B<sub>s</sub> (and M<sub>s</sub>) values indicating higher ferromagnetic phase crystallinity fraction and starting the dominancy of multi-domain magnetization. However there was still remained a significant amount of the amorphous phase. The Group 3 belongs to samples sintered at 1100<sup>0</sup>C (in single-sample sintering) or 1200<sup>0</sup>C (in multi-sample sintering). Stronger ferromagnetic behaviour (B<sub>s</sub>, M<sub>s</sub>) with a diminishing amorphous phase was exhibited in the samples.

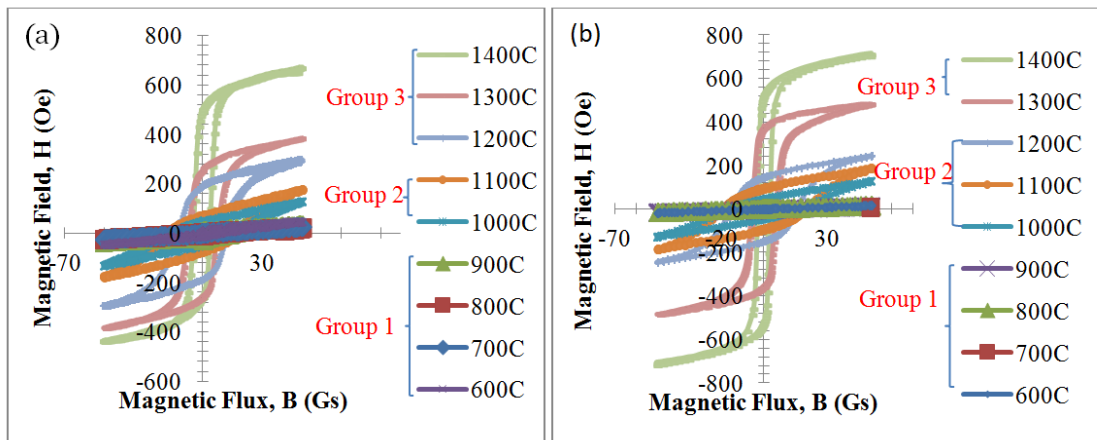


Figure 4: B-H hysteresis loop for single-sample sintered at various temperatures. The circles inside the figure indicate 3 different groups of B-H curve evolution

The H<sub>c</sub> variation in Table 2 shows an increase from 600<sup>0</sup>C to 1100<sup>0</sup>C but decreased from 1100<sup>0</sup>C to 1400<sup>0</sup>C. The H<sub>c</sub> is the property most sensitive to porosity and grain size [9], as well as the anisotropy field. H<sub>c</sub> of the samples is small when they are in their multi-domain state, reaching a maximum value at the critical average grain size for single-domain formation, decreasing further with grain size reduction and becoming

zero when the grains become superparamagnetic [10].

Table 2: B-H loop parameters as a function of grain size at different sintering Temperatures

Sintering temperature (°C)	Single-Sample Sintering				Multi-Sample Sintering			
	Grain Size, ( $\mu\text{m}$ ) $\pm$ 0.01	Saturation induction, $B_s$ (Gs)	Saturation magnetization, $M_s$ ( $\text{emu}/\text{cm}^3$ )	Coercivity, $H_c$ (Oe)	Grain Size, ( $\mu\text{m}$ ) $\pm$ 0.01	Saturation induction, $B_s$ (Gs)	Saturation magnetization, $M_s$ ( $\text{emu}/\text{cm}^3$ )	Coercivity, $H_c$ (Oe)
600	0.16	2.1	1.7	2.6	0.20	16.9	2.2	0.1
700	0.17	2.3	2.6	3.1	0.21	24.9	2.7	0.7
800	0.18	16.4	3.9	6.7	0.25	35.8	4.7	1.3
900	0.28	20.6	4.8	10.9	0.26	49.6	5.2	3.9
1000	0.33	120.7	5.4	15.5	0.28	128.6	5.5	15.8
1100	0.60	173.2	5.7	18.5	0.58	185.7	6.2	19.3
1200	1.14	223.7	10.9	12.4	0.80	244.5	12.8	15.2
1300	1.68	378.9	21.2	7.4	1.25	463.1	23.3	8.8
1400	2.71	570.4	26.3	4.3	3.09	714.6	29.1	2.9

## CONCLUSION

The concise effect of different sintering scheme on morphological and magnetic properties of polycrystalline YIG synthesized by using HEBM technique has been investigated. With a great care experimental procedure, single-sample and multi-sample sintering process yielded highly similar trends of magnetic properties vs microstructure. Microstructural and B-H loop investigations showed that phase purity and grain size strongly influenced the B-H loop shape, and thus segregating them into 3 different groups: weak, moderately strong and strong ferromagnetic. The results strongly suggest that both high reactivity particles produced from high energy milling and human meticulousness contributes to the clear microstructure-magnetic properties evolution trends.

## ACKNOWLEDGEMENTS

We would like to give our great thanks to the Ministry of Higher Education and Universiti Putra Malaysia for financial support of this research.

## REFERENCES

- [1]. I. Fernandez-Garcia, I., M. Suarez, J. L. Menendez, *Journal of Alloys and Compounds*, **495** (2010) 196-199.
- [2]. M. A. Gilleo and S. Geller, *Physical Review*, **110** (1958) 73-78.

- [3]. F. Lamastra, R. Bianco, F. Leonardi, G. Montesperelli, F. Nanni, G. Gusmano, *Materials Chemistry and Physics*. **107** (2008) 274-280.
- [4]. J. S. Kim and W. H. Chang, *Materials Research Bulletin*, **44** (2009) 633–637.
- [5]. H. Gleiter, *Progress in Materials Science*, **33** (1989) 223-315.
- [6]. W.S. Chiu, S. Radimana, R. Abd-Shukor, M.H. Abdullah, P.S. Khiew, *Journal of Alloys and Compounds* **459** (2008) 291–297.
- [7]. P. Vaqueiro, M. A. Lopez-Quintela, J. Rivas, J. M. Greneche, *Journal of Magnetism and Magnetic Materials*, **169** (1997) 56-68.
- [8]. C. P. Bean, *Journal of Applied Physics*, **26** (1955)1381-1383.
- [9]. A. Goldman, Handbook of modern ferromagnetic materials, 2nd ed., United States of America,: Kluwer Academic Publishers, 2002.
- [10]. Cullity, B. D. and Graham, C. D, Introduction to magnetic materials 2<sup>nd</sup> edition. New Jersey: Wiley-IEEE press, 2009.